

# Decentralized Synchronization of Uncertain Nonlinear Systems With a Reputation Algorithm

Justin R. Klotz<sup>1</sup>, Anup Parikh, Teng-Hu Cheng<sup>2</sup>, and Warren E. Dixon, *Fellow, IEEE*

**Abstract**—Decentralized synchronization approaches generally assume that communication of state information between neighboring agents is completely accurate. However, just one agent’s communication of inaccurate information to neighbors can significantly degrade the performance of the entire network. To help abate this problem, we present a decentralized controller for a leader-follower framework which uses local information to vet neighbors and change consensus weights accordingly. Because updates of the consensus weights produce a switched system, switching control theory techniques are used to develop a dwell-time that must elapse between agents’ successive weight updates. A Lyapunov-based stability analysis is presented which develops sufficient conditions for approximate convergence of follower agents’ states to a leader agent’s time-varying state. Simulation results are provided to demonstrate the performance of the developed techniques.

**Index Terms**—Networks of autonomous agents, distributed algorithms/control, nonlinear systems, switched control.

## I. INTRODUCTION

DECENTRALIZED control refers to the cooperation of multiple agents in a network to accomplish a collective task. Networked agents can represent autonomous robotic systems, such as mobile ground robots, unmanned aerial vehicles (UAVs), autonomous underwater vehicles (AUVs), and spacecraft. Compared to centralized control, in which a central agent communicates with all other systems to compute control policies, decentralized control is characterized by local interactions, in which agents coordinate with only a subset of the network to accomplish a network-wide task. The distribution of control policy generation benefits from mitigated computational and bandwidth demand, robustness to communication link failure, and robustness to unexpected agent failure. However, decentralized control suffers from a greater vulnerability to misbehavior of an affected agent. As opposed to centralized control,

in which a central agent can vet any agent in comparison with the rest of the network, decentralized control exhibits less situational awareness in the sense that an agent is only exposed to the actions of its neighbors. Thus, there are fewer checks and balances to discriminate inaccurate information or malevolent behavior, which motivates the development of decentralized methods which evaluate a level of trust for network neighbors.

There are multiple methods for an autonomous vehicle to determine its position, orientation, and velocity, including using GPS, an inertial measurement unit (IMU), and simultaneous localization and mapping (SLAM). However, self-localization may produce inaccurate results. For example, a UAV might poorly estimate its own state as a result of corruption of an IMU, GPS spoofing, GPS jamming (and subsequent use of a less accurate IMU), inaccurate onboard SLAM due to a lack of landscape features, or IMU/GPS/SLAM measurement noise. In addition, heterogeneity in the hardware of the robotic platforms can naturally lead to disparity in the accuracy of agents’ estimates of their own states. Thus, if communication is used in a team of autonomous systems to share state information, care should be taken when using a neighbor’s communicated state in a control policy, especially in the context of decentralized interactions.

Another method to obtain information about agents in the network is neighbor sensing, e.g., use of a camera or radar. Neighbor sensing can provide the relative position of neighboring vehicles; however, it is very reliant on a direct line-of-sight (LOS) between the vehicles. For example, ground vehicles may temporarily lose LOS when navigating around obstructions. In addition, agents may need to distribute neighbor sensing time between multiple neighbors. For example, if a ground vehicle can observe two neighboring vehicles in dissimilar locations with a camera but cannot observe both neighbors at the same time due to a narrow camera field of view, the camera may need to rotate to share observation time between neighbors.

This work considers a decentralized network control scenario in which agents use both communication and neighbor sensing to interact. The communication is assumed to be continuously available, but have possible inaccuracies due to poor self localization. The sensor measurements are assumed to provide accurate relative position information, but only occur intermittently. Because the sensor measurements are modeled as intermittent, and therefore may not be frequent enough to be implemented in closed-loop control, they are used to vet communicated information so that an agent can rely more on information from more reliable neighbors. A trust algorithm is developed in which each agent quantitatively evaluates the trust of each neighbor based on the discrepancy between communicated and sensed information.

Manuscript received July 25, 2016; accepted October 2, 2016. Date of publication October 13, 2016; date of current version March 16, 2018. This work was supported in part by NSF Awards 1161260, 1217908, and the AFRL Mathematical Modeling and Optimization Institute. Any opinions, findings and conclusions or recommendations expressed in this material are those of the authors and do not necessarily reflect the views of the sponsoring agency. Recommended by Associate Editor H. Ishii.

J. R. Klotz and W. E. Dixon are with the Department of Mechanical and Aerospace Engineering, University of Florida, Gainesville FL 32611-6250 USA (e-mail: jklotz@ufl.edu; wdixon@ufl.edu).

A. Parikh is with Sandia National Laboratories, Albuquerque NM 87185 USA (e-mail: anuppari@gmail.com).

T.-H. Cheng is with the Department of Mechanical Engineering, National Chiao Tung University, Hsinchu Taiwan 300 (e-mail: tenghu@nctu.edu.tw).

Color versions of one or more of the figures in this paper are available online at <http://ieeexplore.ieee.org>.

Digital Object Identifier 10.1109/TCNS.2016.2617623

The trust values are used in a reputation algorithm, in which agents communicate about a mutually shared neighbor to collaboratively obtain a reputation. Each agent's contribution to the reputation algorithm is weighted by that neighbor's own reputation. The result of the reputation algorithm is used to update consensus weights which affect the relative weighting in use of a neighbor's communicated information compared to other neighbors', if an agent has multiple neighbors. Note that, although communication and neighbor sensing are used to characterize these two different types of feedback, the approach in this paper applies to any two types of feedback which share the characteristics given here to communication and neighbor sensing.

In this work, the objective for each agent is to perform synchronization (cf. [1]–[5]) to the trajectory of a network leader. The follower agents interact in a network modeled by a strongly connected, directed graph, and the leader agent interacts with only a subset of the follower agents. In comparison with other literature, the recent results in [6]–[8] propose reputation algorithms for networked agents performing decentralized control; however, no convergence analysis is given to guarantee achievement of the control objective with regard to the physical states of the networked systems. One of the difficulties in performing a convergence analysis for a reputation algorithm combined with a decentralized controller is that consensus weight updates can cause discontinuities in the control policy, making the network a switched system, and requiring a dwell-time between updates to the consensus weights (cf. [9]). Furthermore, because consensus weights generally take any value between 0 and 1, there are an infinite number of possible consensus weight combinations in the network, which makes a switched system-based approach difficult: a common Lyapunov function or bounds on a candidate switched Lyapunov function may be difficult to obtain. The insightful work in [9] develops conditions for convergence for a network of agents with single integrator dynamics performing decentralized control with a reputation algorithm. However, the reputation algorithm in [9] inherently requires the control objective to be convergence of all agents' states to a fixed point, which is more restrictive than the general leader-synchronization problem. Additionally, the work in [9] relies on the existence of a dwell-time between consensus weight updates, but an approach to compute a sufficient dwell-time is not discussed. The development in [10] avoids the effects of discontinuities by updating consensus weights smoothly in time based on continuously updated trust values in a network of agents with single integrator dynamics. However, the effects on the performance of the dynamical systems due to varying the consensus weights in time is not addressed. Additionally, the controller in [10] only provides network convergence of the agents' states to a single point, which is a function of the trust values, initial conditions of the agents' states, and the network configuration. The method developed in this paper provides a new decentralized reputation algorithm and controller for synchronization to a time-varying leader trajectory with an associated convergence analysis and sufficient gain conditions for a network of agents with nonlinear second-order dynamics. Additionally, based on the convergence analysis, this work discusses a method to compute a sufficient minimum dwell-time for the switched network system.

Simulation results are provided to demonstrate the performance of the developed reputation algorithm, decentralized controller, and network topology-dependent dwell-time.

## II. PROBLEM FORMULATION

### A. Graph Theory Notation

Consider a leader-follower network composed of a single leader and a finite number  $\mathcal{F} \in \mathbb{Z}_{>0}$  of follower agents. The interaction topology for the follower agents is modeled with a directed graph  $\mathcal{G}_{\mathcal{F}} = \{\mathcal{V}_{\mathcal{F}}, \mathcal{E}_{\mathcal{F}}\}$ , where  $\mathcal{V}_{\mathcal{F}} = \{1, \dots, \mathcal{F}\}$  is the set of enumerated nodes representing the follower agents, and  $\mathcal{E}_{\mathcal{F}} \subseteq \mathcal{V}_{\mathcal{F}} \times \mathcal{V}_{\mathcal{F}}$  is the set of edges which denote interaction links. The follower graph  $\mathcal{G}_{\mathcal{F}}$  is modeled such that the network topology is static, i.e.,  $\mathcal{V}_{\mathcal{F}}$  and  $\mathcal{E}_{\mathcal{F}}$  do not vary in time. The edge  $(j, i)$  belongs to  $\mathcal{E}_{\mathcal{F}}$  if agent  $i \in \mathcal{V}_{\mathcal{F}}$  receives information from agent  $j \in \mathcal{V}_{\mathcal{F}}$ , and  $(i, i) \notin \mathcal{E}_{\mathcal{F}}$  for all  $i \in \mathcal{V}_{\mathcal{F}}$ . The set of neighboring follower agents  $\mathcal{N}_{\mathcal{F}i}$  of an agent  $i \in \mathcal{V}_{\mathcal{F}}$  is defined as  $\mathcal{N}_{\mathcal{F}i} \triangleq \{j \in \mathcal{V}_{\mathcal{F}} \mid (j, i) \in \mathcal{E}_{\mathcal{F}}\}$ . Interaction links are weighted with the values in the adjacency matrix  $A \triangleq [a_{ij}] \in \mathbb{R}^{\mathcal{F} \times \mathcal{F}}$ , where the edge weights  $a_{ij} : \mathbb{R} \rightarrow \mathbb{R}_{>0}$  are time-varying and satisfy  $a_{ij} > 0$  if  $(j, i) \in \mathcal{E}_{\mathcal{F}}$  and  $a_{ij} = 0$  otherwise. The Laplacian matrix  $\mathcal{L}_{\mathcal{F}} \in \mathbb{R}^{\mathcal{F} \times \mathcal{F}}$  of graph  $\mathcal{G}_{\mathcal{F}}$  is defined as  $\mathcal{L}_{\mathcal{F}} \triangleq D - A$ , where  $D \triangleq \text{diag}\{d_1, \dots, d_{\mathcal{F}}\} \in \mathbb{R}^{\mathcal{F} \times \mathcal{F}}$  is the degree matrix with  $d_i \triangleq \sum_{j \in \mathcal{N}_{\mathcal{F}i}} a_{ij}$ . The directed graph which includes the leader agent is constructed as  $\mathcal{G} = \{\mathcal{V}_{\mathcal{F}} \cup L, \mathcal{E}_{\mathcal{F}} \cup \mathcal{E}_L\}$ , where  $L$  denotes the leader agent and the edge  $(L, i)$  belongs to  $\mathcal{E}_L$  if follower agent  $i \in \mathcal{V}_{\mathcal{F}}$  receives information from the leader. The constant leader-connectivity (i.e., pinning) matrix  $B \in \mathbb{R}^{\mathcal{F} \times \mathcal{F}}$  is defined as the diagonal matrix  $B \triangleq \text{diag}\{b_1, \dots, b_{\mathcal{F}}\}$ , where  $b_i > 0$  if  $(L, i) \in \mathcal{E}_L$  and  $b_i = 0$  otherwise. The following assumption specifies the class of networks considered in this paper, where the term “strongly connected” indicates that there exists a sequence of directed edges between any two nodes.

*Assumption 1:* The graph  $\mathcal{G}_{\mathcal{F}}$  is strongly connected and at least one agent is connected to the leader.

### B. Dynamic Models and Properties

Let the dynamics of each follower agent  $i \in \mathcal{V}_{\mathcal{F}}$  be modeled with uncertain second-order nonlinear dynamics as

$$\ddot{x}_i = f_i(x_i, \dot{x}_i) + u_i \quad (1)$$

where  $x_i \in \mathbb{R}^m$  is the state,  $f_i : \mathbb{R}^m \times \mathbb{R}^m \rightarrow \mathbb{R}^m$  denotes the uncertain, first-order differentiable, nonlinear drift dynamics, and  $u_i \in \mathbb{R}^m$  is the control input to be designed. The time-varying trajectory of the leader state is denoted by  $x_L : \mathbb{R} \rightarrow \mathbb{R}^m$ , which is communicated to at least one of the follower agents. The following assumptions concerning the follower agents' dynamics and the leader trajectory are made to simplify the analysis.

*Assumption 2:* The leader state trajectory is sufficiently smooth such that  $x_L, \dot{x}_L, \ddot{x}_L$  are bounded.

Note that the dynamics in (1) can be represented in Euler-Lagrange form if the inertia matrix is known and used in the controller. The inertia matrix is omitted from the dynamics to simplify the subsequent analysis.

### C. Neighbor Communication and Sensing

Neighboring follower agents use both communication and sensing to interact with each other. Communication of continuous estimates of the state information  $(x_j, \dot{x}_j)$  of agent  $j \in \mathcal{V}_{\mathcal{F}}$  is available to its neighbor  $i \in \mathcal{N}_{\mathcal{F}j}$  at all times; however, the communicated state estimates may be inaccurate due to imperfect knowledge of the agent's own state in the global coordinate system (i.e., the act of communication itself is not responsible for inaccuracy of communicated information). For example, a UAV in a network may transmit an inaccurate estimate of its own position due to imperfect navigation. However, intermittent neighbor sensing of an agent  $j \in \mathcal{V}_{\mathcal{F}}$  by a neighbor  $i \in \mathcal{N}_{\mathcal{F}j}$  provides accurate relative position information  $(x_j - x_i)$  at isolated points in time. For example, an agent may be able to observe neighbors using a camera, but may only determine the relative position intermittently due to occlusions, low hardware refresh rates, etc. As a consequence, neighbor sensing may not be frequent enough for stability in a control algorithm which uses neighbor sensing alone. Thus, each agent must use both continuous, possibly inaccurate neighbor communication and accurate, intermittent neighbor sensing to accomplish a control objective. Because the intermittent neighbor sensing is accurate, it may be used to vet and intelligently use the communicated state information. Let  $\hat{x}_i, \dot{\hat{x}}_i$  denote the estimates of  $x_i, \dot{x}_i$  computed by agent  $i \in \mathcal{V}_{\mathcal{F}}$ . The following assumptions concerning the communicated state information are made to facilitate the following analysis, where  $\|\cdot\|$  denotes the Euclidean norm.

*Assumption 3:* The difference between the estimated state information  $\hat{x}_i, \dot{\hat{x}}_i$  and the actual state information  $x_i, \dot{x}_i$  is bounded for each follower agent  $i \in \mathcal{V}_{\mathcal{F}}$ , i.e., there exist known positive constants  $b_x, b_{\dot{x}} \in \mathbb{R}$  such that  $\|\hat{x}_i - x_i\| \leq b_x$  and  $\|\dot{\hat{x}}_i - \dot{x}_i\| \leq b_{\dot{x}}$  for each  $i \in \mathcal{V}_{\mathcal{F}}$  and all time.

*Assumption 4:* State estimates communicated from the leader agent are accurate.

As seen in the following section, Assumption 4 is critical to achieving close synchronization with the leader. Whereas it may be difficult to guarantee perfect state communication for each agent, it is plausible to guarantee Assumption 4 by outfitting only the leader agent with more robust localization equipment or monitoring by personnel.

### D. Control Objective

Similar to traditional synchronization approaches (cf. [1]–[4]), the objective is to drive the states of the networked agents towards the state of the network leader such that  $\limsup_{t \rightarrow \infty} \|x_i(t) - x_L(t)\| \leq \varepsilon$  with a small  $\varepsilon$  through advantageous use of the communicated and sensed information.

## III. CONTROLLER DEVELOPMENT

Before the developed control policy is presented, its constituent trust metric, reputation algorithm, edge weight update policy, and error signals are presented.

### A. Trust Metric

Each agent  $i \in \mathcal{V}_{\mathcal{F}}$  assigns a trust value,  $\sigma_{ij} \in [0, 1]$ , to each neighbor  $j \in \mathcal{N}_{\mathcal{F}i}$ , where 0 corresponds to no trust and 1 cor-

responds to high trust. The trust value is computed using communicated information  $\hat{x}_j$ , internal information  $\hat{x}_i$ , and sensed relative position information  $x_j - x_i$  from time instances when sensor measurements are available. Let  $t_{ij}^1, t_{ij}^2, \dots \in \mathbb{R}$  denote the time instances in which agent  $i$  obtains a sensor measurement of  $x_j - x_i$ , let  $\bar{t} \in \mathbb{R}$  denote a positive number, and let  $S_{ij}(t) \triangleq \{t_{ij}^l \mid (l \in \mathbb{Z}_{>0}) \wedge (t - \bar{t} \leq t_{ij}^l \leq t)\}$  denote the set of neighbor sensing time instances which have occurred after  $t - \bar{t}$  up until the current time.<sup>1</sup> The use of  $\bar{t}$  is motivated by expiring relevancy of old neighbor sensing data and mitigation of computational burden in determining a trust value (cf. [11]). There are numerous options in selecting a trust metric (see the survey in [12]), and any trust metric which maps into  $(0, 1]$  and has a positive lower bound for a bounded input is appropriate for the analysis developed in this paper. In this work, a trust metric is designed as

$$\sigma_{ij} \triangleq \begin{cases} 1 & |S_{ij}| = 0 \\ \frac{1}{|S_{ij}|} \sum_{t_{ij}^l \in S_{ij}} e^{-s \|\tilde{x}_{ij}(t_{ij}^l) - \hat{\tilde{x}}_{ij}(t_{ij}^l)\|} & \text{otherwise} \end{cases} \quad (2)$$

where  $s \in \mathbb{R}$  is a positive tuning parameter,  $\tilde{x}_{ij} \triangleq x_j - x_i$  is the relative position obtained via neighbor sensing, and  $\hat{\tilde{x}}_{ij} \triangleq \hat{x}_j - \hat{x}_i$  is the relative position obtained via communication of the state estimate  $\hat{x}_j$  and the internal position estimate  $\hat{x}_i$  maintained by agent  $i$ .<sup>2</sup> In (2), a trust value of 1 is computed if there are no recent sensor measurements (i.e.,  $S_{ij}(t)$  is an empty set). If there are recent sensor measurements, the term  $e^{-s \|\tilde{x}_{ij}(t_{ij}^l) - \hat{\tilde{x}}_{ij}(t_{ij}^l)\|}$  maps the discrepancy between the estimated relative position and the actual relative position to  $(0, 1]$ . The result is then averaged with the corresponding values for the other sensor measurements to obtain the overall trust value. Note that  $\tilde{x}_{ij}$  and  $\hat{\tilde{x}}_{ij}$  may differ due to an inaccurate estimate of  $\hat{x}_i$ , i.e., an agent's trust of a neighbor may be affected by an inaccurate estimate of its own state. Future work may investigate methods to better estimate an agent's own state based on neighbor feedback.

### B. Reputation Algorithm

The trust values,  $\sigma_{ij}$ , described in the preceding section are not used directly to update consensus weights; rather, trust values are used to help develop an overall reputation of a neighbor. Each follower agent  $i \in \mathcal{V}_{\mathcal{F}}$  maintains a reputation value<sup>3</sup>  $\zeta_{ij} : \Pi_{l=1}^{2|\mathcal{N}_{\mathcal{F}i} \cap \mathcal{N}_{\mathcal{F}j}|+2} \mathbb{R} \rightarrow \mathbb{R}$  for every neighbor  $j \in \mathcal{N}_{\mathcal{F}i}$  based on trust of neighbor  $j$  and recommendations from mutual neighbors, where the reputation is updated using trust values and recommendations as

$$\dot{\zeta}_{ij} = \sum_{n \in \mathcal{N}_{\mathcal{F}i} \cap \mathcal{N}_{\mathcal{F}j}} \eta_{\zeta i} \zeta_{in} (\zeta_{nj} - \zeta_{ij}) + \eta_{\sigma i} (\sigma_{ij} - \zeta_{ij}) \quad (3)$$

with the initial condition  $\zeta_{ij}(0) = 1$ , where a higher reputation corresponds to higher reliability, and  $\eta_{\zeta i}, \eta_{\sigma i} \in \mathbb{R}_{>0}$  are

<sup>1</sup> Recall that sensor measurements occur at isolated points in time, i.e.,  $S_{ij}(t)$  is a finite set for all  $t \in \mathbb{R}$ .

<sup>2</sup> Similar to [11], the summation in (2) can be weighted by how much time has elapsed since the measurements took place, if relevant for the intended application.

<sup>3</sup> In this context, the symbol  $\Pi$  denotes the indicated number of Cartesian products.

tunable gains that weigh how much recommended information (i.e.,  $\zeta_{nj}$ ) is relied upon compared to directly observed information (i.e.,  $\sigma_{ij}$ ). The first term in (3) contributes towards the reputation update by agent  $i$  for agent  $j$  based on the reputation of  $j$  held by mutual neighbors  $n \in \mathcal{N}_{\mathcal{F}_i} \cap \mathcal{N}_{\mathcal{F}_j}$  via communication. The contribution of a mutual neighbor to the reputation update is weighted by the reputation of that agent, as seen in the multiplication by  $\zeta_{in}$ . Thus, an agent which has a low reputation has less significant impact in recommendation of a reputation value. The second term in (3) directly uses the observation-based trust value to update reputation. A simple analysis shows that, for each connection  $(j, i) \in \mathcal{E}_{\mathcal{F}}$ , the reputation value  $\zeta_{ij}$  is bounded such that  $\zeta_{ij} \in [\underline{\sigma}^*, 1]$  for all  $t \in \mathbb{R}$ , where  $\underline{\sigma}^* \in \mathbb{R}$  is a bounding constant such that  $\sigma_{ij} \geq \underline{\sigma}^*$  for all  $t \in \mathbb{R}$ , and  $\underline{\sigma}^* > 0$  by Assumption 3. Also, note that a reputation value  $\zeta_{ij}$  can be communicated accurately; whereas an agent may communicate inaccurate state estimate information  $\hat{x}_i, \hat{\hat{x}}_i$  due to imperfectly knowing its own state, each agent is able to transmit reputation values without error.

*Remark 1:* Compared to [6], when an agent computes a neighbor's reputation, the reputation algorithm in (3) incorporates that agent's trust of that neighbor. Compared to [7] and [10], this reputation algorithm weights neighbor recommendations by their reputations and can weigh how much recommended information is relied upon compared to directly observed information. Compared to [8], this algorithm incorporates dynamic trust measurements into the agents' reputations. Finally, the trust algorithm in [9] is based on rejection of extreme state values, is only designed for the consensus of agents' states towards a fixed point, and does not perform propagation of trust values.

### C. Edge Weight Updates and Timing

Edge weights are often used to describe relative levels of influence of an agent's neighbors on its control policy. The reputation values,  $\zeta_{ij}$ , are used to update edge weight values,  $a_{ij}$ , which quantify how much influence a neighbor has in the subsequently developed decentralized control policy. However, changes to the edge weight values in the control policy can affect the stability of the closed-loop system. To control the effects of the edge weight updates on the systems' feedback, and based on the subsequent convergence analysis, the edge weights are updated at discrete times in predefined time intervals. Thus, the adjacency matrix  $A$  and the Laplacian matrix  $\mathcal{L}_{\mathcal{F}}$  are functions of time, i.e.,  $A : \mathbb{R} \rightarrow \mathbb{R}^{\mathcal{F} \times \mathcal{F}}$  and  $\mathcal{L}_{\mathcal{F}} : \mathbb{R} \rightarrow \mathbb{R}^{\mathcal{F} \times \mathcal{F}}$ , where the adjacency matrix is initialized such that  $a_{ij}(0) = \frac{1}{|\mathcal{N}_{\mathcal{F}_i}|}$  if  $(j, i) \in \mathcal{E}_{\mathcal{F}}$ , i.e., all follower-to-follower connections are equally weighted at  $t = 0$ . However, if the edge weights are updated too rapidly, then the resulting frequent discontinuities in the switched closed-loop system may cause instability (cf. [13, Chapter 2]). Thus, a dwell-time (cf. [13, Chapter 3]),  $\tau_d \in \mathbb{R}_{>0}$ , is subsequently developed to describe the minimum amount of time that must elapse before an agent  $i \in \mathcal{V}_{\mathcal{F}}$  can update its edge weight values,  $\{a_{ij} \mid j \in \mathcal{N}_{\mathcal{F}_i}\}$ , since its last update (or the initial time), and is computed before the control implementation. Implementation of the dwell-time is decentralized in the sense that an agent may

update its edge weights at different times from other neighbors as long as the elapsed time between successive updates of that agent's own weights is not shorter than the dwell-time. The network topology-dependent minimum dwell-time is given in Section VI and is based on the subsequent convergence analysis.

Let  $t_{di}^1, t_{di}^2, \dots \in \mathbb{R}$  denote the times at which agent  $i \in \mathcal{V}_{\mathcal{F}}$  updates its edge weight values  $\{a_{ij} \mid j \in \mathcal{N}_{\mathcal{F}_i}\}$ , where  $t_{di}^{l+1} - t_{di}^l \geq \tau_d$  for all  $l \in \mathbb{Z}_{>0}$ . The edge weights stay constant between updates and the reputation values are mapped to the edge weight values at each update time as

$$a_{ij}(t_{di}^l) = \frac{\zeta_{ij}(t_{di}^l)}{\sum_{n \in \mathcal{N}_{\mathcal{F}_i}} \zeta_{in}(t_{di}^l)}, \quad l \in \mathbb{Z}_{>0} \quad (4)$$

where the reputation values are normalized in (4) so that  $\sum_{j \in \mathcal{N}_{\mathcal{F}_i}} a_{ij} = 1$ . Note that since  $\zeta_{ij} \geq \underline{\sigma}^*$  for all  $(j, i) \in \mathcal{E}_{\mathcal{F}}$  and  $t \in \mathbb{R}$ , there exists a constant  $\underline{a}^* \in \mathbb{R}$  such that  $0 < \underline{a}^* < 1$  and  $a_{ij} \in [\underline{a}^*, 1]$  for all  $(j, i) \in \mathcal{E}_{\mathcal{F}}$  and  $t \in \mathbb{R}$ .

### D. Error Signals

The neighborhood error signal in decentralized control traditionally has the form  $\sum_{j \in \mathcal{N}_{\mathcal{F}_i}} a_{ij}(x_j - x_i) + b_i(x_L - x_i)$ . However, since accurate state information is not always available to each agent, a decentralized neighbor-based error signal is developed using the edge weight updates in (4) and communicated information as

$$\hat{e}_i \triangleq \sum_{j \in \mathcal{N}_{\mathcal{F}_i}} a_{ij}(\hat{x}_j - \hat{x}_i) + b_i(x_L - \hat{x}_i). \quad (5)$$

In (5), the first term provides communication-based feedback for comparison to neighboring follower agents and the second term provides communication-based feedback for comparison to the leader agent, if that connection exists. Hence, instead of imposing discontinuities on the error signal by using the accurate sensed relative state whenever a sensor measurement is available, the strategy is to use the communicated information for feedback and update the edge weights  $a_{ij}$  based on the discrepancy between the communicated and sensed information, as described in Section III-B. The edge weights are updated so that neighbors which seem to provide more accurate information have a greater impact on the synchronization performance.

Because second-order dynamics are considered, an auxiliary error signal is analogously defined as

$$\hat{r}_i \triangleq \sum_{j \in \mathcal{N}_{\mathcal{F}_i}} a_{ij}(\dot{\hat{x}}_j - \dot{\hat{x}}_i) + b_i(\dot{x}_L - \dot{\hat{x}}_i) + \lambda \hat{e}_i \quad (6)$$

where  $\lambda \in \mathbb{R}$  is a constant positive tuning parameter.

### E. Decentralized Controller

The auxiliary error signal in (6) is used to design a piecewise continuous decentralized controller as

$$u_i = k \hat{r}_i \quad (7)$$

where  $k \in \mathbb{R}$  is a constant positive control gain. The following section demonstrates how the discrepancies between communicated and sensed information are advantageously used in the control method in (7).

#### IV. CLOSED-LOOP ERROR SYSTEM

To facilitate analysis of the stability of the closed-loop system, the operator  $\mathcal{P} : \mathbb{R}^{\mathcal{F} \times \mathcal{F}} \rightarrow \mathbb{R}^{\mathcal{F} \times \mathcal{F}}$  is defined as the (positive definite and symmetric) solution to the continuous algebraic Lyapunov Equation (CALE) such that  $M^T \mathcal{P} (M) + \mathcal{P} (M) M = -I_{\mathcal{F}}$  for a Hurwitz matrix  $M \in \mathbb{R}^{\mathcal{F} \times \mathcal{F}}$ , where  $I$  indicates the identity matrix of the denoted dimension.

*Lemma 1:* If Assumption 1 is satisfied, then the matrix  $-\mathcal{L}_{\mathcal{F}} - B$  is Hurwitz.

*Proof:* See the Appendix.  $\blacksquare$

For convenience, the vectors  $x_i$ ,  $\hat{x}_i$ , and  $x_L$  are stacked such that  $X \triangleq [x_1^T, \dots, x_{\mathcal{F}}^T]^T \in \mathbb{R}^{\mathcal{F}m}$ ,  $\hat{X} \triangleq [\hat{x}_1^T, \dots, \hat{x}_{\mathcal{F}}^T]^T \in \mathbb{R}^{\mathcal{F}m}$ ,  $X_L \triangleq [x_L^T, \dots, x_L^T]^T \in \mathbb{R}^{\mathcal{F}m}$ . To facilitate the description of the agents' progress towards synchronization, the error signals  $E \triangleq X_L - X \in \mathbb{R}^{\mathcal{F}m}$  and  $R \triangleq \dot{E} + \lambda E \in \mathbb{R}^{\mathcal{F}m}$  are introduced. Using the dynamics in (1), the controller in (7), and the definitions of  $E$  and  $R$ , the closed-loop dynamics can be represented as

$$\begin{aligned} \dot{R} &= \ddot{X}_L - F(X, \dot{X}) + \lambda \dot{E} - k((\mathcal{L}_{\mathcal{F}} + B) \otimes I_m) R \\ &\quad + k((\mathcal{L}_{\mathcal{F}} + B) \otimes I_m) (\dot{\hat{X}} - \dot{X} + \lambda (\hat{X} - X)) \end{aligned} \quad (8)$$

where  $F \triangleq [f_1^T, \dots, f_{\mathcal{F}}^T]^T \in \mathbb{R}^{\mathcal{F}m}$  and the second line in (8) isolates the effects of inaccurate state estimation on the closed-loop system. After some algebraic manipulation, (8) can be expressed as

$$\begin{aligned} \dot{R} &= N_d + \tilde{N} - k((\mathcal{L}_{\mathcal{F}} + B) \otimes I_m) R \\ &\quad - (\mathcal{P}(-\mathcal{L}_{\mathcal{F}} - B) \otimes I_m)^{-1} E \\ &\quad + k((\mathcal{L}_{\mathcal{F}} + B) \otimes I_m) (\dot{\hat{X}} - \dot{X} + \lambda (\hat{X} - X)) \end{aligned} \quad (9)$$

where the functions  $N_d : \prod_{i=1}^3 \mathbb{R}^{\mathcal{F}m} \rightarrow \mathbb{R}^{\mathcal{F}m}$  and  $\tilde{N} : \prod_{i=1}^6 \mathbb{R}^{\mathcal{F}m} \rightarrow \mathbb{R}^{\mathcal{F}m}$  are defined as  $N_d \triangleq \dot{X}_L - F(X_L, \dot{X}_L)$  and  $\tilde{N} \triangleq F(X_L, \dot{X}_L) - F(X, \dot{X}) + \lambda \dot{E} + (\mathcal{P}(-\mathcal{L}_{\mathcal{F}} - B) \otimes I_m)^{-1} E$ . Terms are segregated into  $N_d$  and  $\tilde{N}$  such that  $\|N_d\|$  can be upper-bounded through Assumption 2 by a constant and  $\|\tilde{N}\|$  can be upper-bounded by a function of the error signals  $E$  and  $R$  through a Mean Value Theorem-based approach, where the matrix  $(\mathcal{P}(-\mathcal{L}_{\mathcal{F}} - B))^{-1}$  is upper bounded by a constant, as shown in the following section. Accordingly, let the known constant  $\bar{N}_d \in \mathbb{R}$  be defined such that

$$\sup_{t \in \mathbb{R}} \|N_d\| \leq \bar{N}_d. \quad (10)$$

Additionally, because the drift dynamics are first-order differentiable, by [14, Lemma 5], there exists a strictly increasing, radially unbounded function  $\rho : \mathbb{R} \rightarrow \mathbb{R}$  which facilitates an upper bound for  $\|\tilde{N}\|$  as

$$\|\tilde{N}\| \leq \rho(\|Z\|) \|Z\| \quad (11)$$

where the composite vector  $Z \in \mathbb{R}^{2\mathcal{F}m}$  is defined as  $Z \triangleq [E^T, R^T]^T$ .

#### V. CONVERGENCE ANALYSIS

Some additional expressions are introduced to facilitate the convergence analysis. Let the set  $\mathcal{P}$  be defined as  $\mathcal{P} \triangleq \left\{ \mathcal{P}(-\mathcal{L}_{\mathcal{F}} - B) \mid a_{ij} \in [\underline{a}^*, 1], \sum_{j \in \mathcal{N}_{F_i}} a_{ij} = 1, \forall (j, i) \in \mathcal{E}_{\mathcal{F}} \right\}$ , which is the set of solutions for the CALE for every possible value of the matrix  $-\mathcal{L}_{\mathcal{F}} - B$  under the edge weight update law in (4). Because  $\mathcal{P}$  is a bounded set, there exist positive constants  $\underline{p}^*, \bar{p}^* \in \mathbb{R}$  defined as  $\underline{p}^* \triangleq \inf_{P \in \mathcal{P}} \underline{\lambda}(P)$  and  $\bar{p}^* \triangleq \sup_{P \in \mathcal{P}} \bar{\lambda}(P)$ , where  $\underline{\lambda}(\cdot), \bar{\lambda}(\cdot)$  denote the minimum and maximum eigenvalues, respectively. These constants are used to define a minimum sufficient dwell-time,  $\tau_d^* \in \mathbb{R}$ , which is designed for use in the convergence theorem as

$$\tau_d^* \triangleq \frac{\ln(\mu^*)}{\frac{\psi}{\max\{\bar{p}^*, 1\}} - \beta^*}$$

where the positive constants  $\psi, \mu^* \in \mathbb{R}$  are defined as  $\psi \triangleq \frac{1}{2} \min\{\lambda, \frac{k}{4}\}$  and  $\mu^* \triangleq \frac{\max\{\bar{p}^*, 1\}}{\min\{\underline{p}^*, 1\}}$ , and  $\beta^* \in \mathbb{R}$  is a selectable positive constant which satisfies  $0 < \beta^* < \frac{\psi}{\max\{\bar{p}^*, 1\}}$ . As shown in the following convergence analysis, there is a tradeoff in the selection of  $\beta^*$  between convergence rate and how rapidly the agents may update their edge weights.

To further facilitate the subsequent analysis, let the open and connected set  $\mathcal{D}$  be defined as  $\mathcal{D} \triangleq \{Z \in \mathbb{R}^{2\mathcal{F}m} \mid \|Z\| < \chi^*\}$ , where  $\chi^* \triangleq \inf\left(\rho^{-1}\left(\left[\frac{1}{\bar{p}^*} \sqrt{\frac{k\psi}{3}}, \infty\right)\right)\right) \in \mathbb{R}$  and the inverse image  $\rho^{-1}(\Theta) \subset \mathbb{R}$  for a set  $\Theta \subset \mathbb{R}$  is defined as  $\rho^{-1}(\Theta) \triangleq \{\xi \in \mathbb{R} \mid \rho(\xi) \in \Theta\}$ . The set of stabilizing initial conditions is a subset of  $\mathcal{D}$  and is defined as

$$\mathcal{S} \triangleq \left\{ Z \in \mathbb{R}^{2\mathcal{F}m} \mid \|Z\| < \frac{\chi^*}{\mu^*} \right\}. \quad (12)$$

Finally, the constant parameter  $\bar{\mathcal{L}}_B \in \mathbb{R}$  is defined as  $\bar{\mathcal{L}}_B \triangleq \sqrt{|\mathcal{E}_{\mathcal{F}}| + \mathcal{F} + \sum_{i \in \mathcal{V}_{\mathcal{F}}} b_i^2}$  to upper bound  $\|\mathcal{L}_{\mathcal{F}}(t) + B\|$  for any combination of allowed edge weights, since  $\|\mathcal{L}_{\mathcal{F}}(t) + B\| \leq \|\mathcal{L}_{\mathcal{F}}(t) + B\|_F \leq \bar{\mathcal{L}}_B$  for all  $t \in \mathbb{R}$  by the triangle inequality and the fact that  $0 < a_{ij} \leq 1$ ,  $a_{ii} = 0$  for all  $i, j \in \mathcal{V}_{\mathcal{F}}$ , where  $\|\cdot\|_F$  denotes the Frobenius norm.

The following theorem describes sufficient conditions for the approximate convergence of the follower agents' states towards the leader's state under the decentralized control policy in (7).

*Theorem 1:* For every follower agent  $i \in \mathcal{V}_{\mathcal{F}}$ , the decentralized controller in (7) using the edge weight update policy in (4) provides uniformly ultimately bounded leader synchronization for a network of agents with nonlinear dynamics described in (1) and neighbor communication and sensing feedback described in Section II-C for all initial conditions  $Z(0) \in \mathcal{S}$  in the sense that  $\limsup_{t \rightarrow \infty} \|x_i(t) - x_L(t)\| \leq \varepsilon$  for some  $\varepsilon \in \mathbb{R}_{>0}$ , provided that Assumptions 1–4 are satisfied, the user-selected dwell-time  $\tau_d$  satisfies  $\tau_d \geq \tau_d^*$ , and the state estimate errors are sufficiently

small such that there exists a selection for the gain  $k$  which satisfies the inequality

$$\frac{3(\bar{p}^* \bar{N}_d)^2}{k} + 3k(\bar{p}^* \bar{\mathcal{L}}_B(b_{\dot{x}} + \lambda b_x))^2 < \frac{\psi \chi^*}{\mu^* \max\{\bar{p}^*, 1\}}. \quad (13)$$

*Remark 2:* The inequality in (13) can be satisfied for sufficiently small estimate error upper bounds  $b_x, b_{\dot{x}}$ ; however, as intuition would indicate, stability is not guaranteed for arbitrarily large estimate error upper bounds. Future research may overcome this restriction by developing an algorithm which severs neighbor connections if the apparent error in the communicated state estimates exceeds a threshold, i.e.,  $a_{ij} \neq 0$  if and only if  $(j, i) \in \mathcal{E}_{\mathcal{F}}$  and  $\sigma_{ij} > \sigma_T$ , where  $\sigma_T \in (0, 1)$  is a threshold parameter.

*Proof:* Let the set  $\{t_d^0, t_d^1, \dots\}$  be defined as the union of the switching instances by each agent, including the initial time, such that  $t_d^{l+1} > t_d^l$  for all  $l \in \mathbb{Z}_{\geq 0}$ . Additionally, let the mapping  $\Lambda : [0, \infty) \rightarrow \mathbb{Z}_{\geq 0}$  be defined such that  $\Lambda(t)$  is the number of switches that have occurred until time  $t$ , i.e.,  $\Lambda(t) \triangleq \arg \min_{l \in \mathbb{Z}_{\geq 0}} \{t - t_d^l \mid t - t_d^l \geq 0\}$ . A candidate multiple Lyapunov function,  $V_L : \mathcal{D} \times \mathbb{R} \rightarrow \mathbb{R}$  is defined as

$$V_L(Z, t) \triangleq W_{\Lambda(t)}(Z)$$

where the function  $W_l : \mathcal{D} \rightarrow \mathbb{R}$  belongs to a family of Lyapunov-like functions  $\{W_l \mid l \in \mathbb{Z}_{\geq 0}\}$  defined as  $W_l(Z) \triangleq \frac{1}{2} E^T E + \frac{1}{2} R^T (\mathcal{P}(-\mathcal{L}_{\mathcal{F}}(t_d^l) - B) \otimes I_m) R$ , which satisfies the inequalities

$$\frac{1}{2} \min\{\bar{p}^*, 1\} \|Z\|^2 \leq W_l(Z) \leq \frac{1}{2} \max\{\bar{p}^*, 1\} \|Z\|^2 \quad (14)$$

for all  $Z \in \mathbb{R}^{2\mathcal{F}m}$  and  $l \in \mathbb{Z}_{\geq 0}$ . Using the closed-loop error system in (9), the derivative of  $V_L$  can be expressed as

$$\begin{aligned} \dot{V}_L &= E^T (R - \lambda E) + R^T \left( \mathcal{P} \left( -\mathcal{L}_{\mathcal{F}} \left( t_d^{\Lambda(t)} \right) - B \right) \otimes I_m \right) \\ &\quad \cdot \left( N_d + \tilde{N} - \left( \mathcal{P} \left( -\mathcal{L}_{\mathcal{F}} \left( t_d^{\Lambda(t)} \right) - B \right) \otimes I_m \right)^{-1} E \right. \\ &\quad + k \left( \left( -\mathcal{L}_{\mathcal{F}} \left( t_d^{\Lambda(t)} \right) - B \right) \otimes I_m \right) R \\ &\quad + k \left( \left( \mathcal{L}_{\mathcal{F}} \left( t_d^{\Lambda(t)} \right) + B \right) \otimes I_m \right) \\ &\quad \left. \cdot \left( \dot{\hat{X}} - \dot{X} + \lambda \left( \hat{X} - X \right) \right) \right) \end{aligned}$$

for all  $t \in [t_d^l, t_d^{l+1})$ . After using the definitions of  $\bar{p}^*$ ,  $\bar{p}^*$ , and  $\bar{\mathcal{L}}_B$ , the relationship

$$\begin{aligned} &k R^T (\mathcal{P}(-\mathcal{L}_{\mathcal{F}} - B) (-\mathcal{L}_{\mathcal{F}} - B) \otimes I_m) R \\ &= \frac{k}{2} R^T \left[ (\mathcal{P}(-\mathcal{L}_{\mathcal{F}} - B) (-\mathcal{L}_{\mathcal{F}} - B)) \otimes I_m \right. \\ &\quad \left. + \left( (-\mathcal{L}_{\mathcal{F}} - B) \right)^T \mathcal{P}(-\mathcal{L}_{\mathcal{F}} - B) \right] \otimes I_m R \\ &= -\frac{k}{2} \|R\|^2 \end{aligned}$$

the bounding expressions in (10) and (11), canceling terms, and using the negative feedback of  $R$  to perform nonlinear damping,

$\dot{V}_L$  can be upper-bounded as

$$\begin{aligned} \dot{V}_L &\leq -\lambda \|E\|^2 - \frac{k}{4} \|R\|^2 + \frac{3(\bar{p}^* \rho(\|Z\|) \|Z\|)^2}{k} \\ &\quad + \frac{3(\bar{p}^* \bar{N}_d)^2}{k} + 3k(\bar{p}^* \bar{\mathcal{L}}_B(b_{\dot{x}} + \lambda b_x))^2 \end{aligned}$$

for all  $t \in [t_d^l, t_d^{l+1})$ , where  $b_x$  and  $b_{\dot{x}}$  are defined in Assumption 3. By using the definition of the auxiliary constant  $\psi$ , Assumption 3, and the triangle inequality,  $\dot{V}_L$  is then upper-bounded as

$$\dot{V}_L \leq -\psi \|Z\|^2 - \left( \psi - \frac{3(\bar{p}^* \rho(\|Z\|))^2}{k} \right) \|Z\|^2 + \varepsilon_1$$

for all  $t \in [t_d^l, t_d^{l+1})$ , where the constant  $\varepsilon_1 \in \mathbb{R}$  is defined as  $\varepsilon_1 \triangleq \frac{3(\bar{p}^* \bar{N}_d)^2}{k} + 3k(\bar{p}^* \bar{\mathcal{L}}_B(b_{\dot{x}} + \lambda b_x))^2$ . Provided the initial condition satisfies  $Z(0) \in \mathcal{S}$ , then

$$\dot{V}_L \leq -\psi \|Z\|^2 + \varepsilon_1$$

for all  $t \in [t_d^l, t_d^{l+1})$ . By using the right-side inequality in (14), the upper bound of  $\dot{V}_L$  can be expressed as

$$\dot{V}_L \leq -\frac{\psi}{\max\{\bar{p}^*, 1\}} V_L \quad \forall V_L \geq \frac{\max\{\bar{p}^*, 1\}}{\psi} \varepsilon_1 \quad (15)$$

for all  $t \in [t_d^l, t_d^{l+1})$ . Using the comparison lemma (cf. [15, Lemma 3.4]) with the inequality in (15),  $V_L$  can be shown to be upper-bounded as

$$V_L(Z, t) \leq \max \left\{ e^{-\frac{\psi}{\max\{\bar{p}^*, 1\}}(t-t_d^l)} V_L(Z(t_d^l), t_d^l), \frac{\max\{\bar{p}^*, 1\}}{\psi} \varepsilon_1 \right\} \quad (16)$$

for all  $t \in [t_d^l, t_d^{l+1})$ . By using (16), the ultimate bound of the trajectory of  $V_L$  can be determined by considering the following three cases, where the constant  $\varepsilon_2 \in \mathbb{R}$  is defined as  $\varepsilon_2 \triangleq \frac{\max\{\bar{p}^*, 1\}}{\psi} \varepsilon_1$  (where  $\psi$  is a previously defined gain-dependent term), and  $B_r \subset \mathbb{R}^{2\mathcal{F}m}$  denotes a closed ball of radius  $r \in \mathbb{R}_{>0}$  centered about the origin.

## V. Case I

The trajectory of  $V_L$  has not entered  $B_{\varepsilon_2}$ .

Consider that at time  $t' \in [t_d^l, t_d^{l+1})$ ,  $\{V_L(Z, t) \mid t \leq t'\} \cap B_{\varepsilon_2} = \emptyset$ . The inequality in (16) can be conservatively upper-bounded to account for the effects of switches as

$$\begin{aligned} V_L(Z(t'), t') &\leq e^{-\frac{\psi(t'-t_d^l)}{\max\{\bar{p}^*, 1\}}} \mu^* W_{l-1}(Z(t_d^l)) \\ &\leq e^{-\frac{\psi(t'-t_d^l)}{\max\{\bar{p}^*, 1\}}} \mu^* e^{-\frac{\psi(t_d^l - t_d^{l-1})}{\max\{\bar{p}^*, 1\}}} W_{l-1}(Z(t_d^{l-1})) \\ &\leq \dots \\ &\leq e^{-\frac{\psi t'}{\max\{\bar{p}^*, 1\}}} (\mu^*)^l W_0(Z(0)). \end{aligned} \quad (17)$$

By use of a minimum dwell-time, (17) may be upper-bounded as

$$V_L(Z(t'), t') \leq e^{-\beta^* t'} W_0(Z(0)) \quad (18)$$

if the dwell-time between switching events is greater than or equal to  $\tau_d^*$ . Given (16) and (18), it is clear that use of a dwell-time  $\tau_d \geq \tau_d^*$  guarantees that  $V_L$  is upper-bounded by an exponential decay from the initial condition  $V_L(Z(0), 0)$  towards  $B_{\varepsilon_2}$  for any  $t' \in [t_d^l, t_d^{l+1})$  such that  $\{V_L(Z, t) \mid t \leq t'\} \cap B_{\varepsilon_2} = \emptyset$ .

### V. Case 2

The trajectory of  $V_L$  has reached, or started in, the ball  $B_{\varepsilon_2}$ , and no switch has occurred since entering  $B_{\varepsilon_2}$ .

Consider that  $V_L(Z(t'), t') \in B_{\varepsilon_2}$  at a time  $t' \in [t_d^l, t_d^{l+1})$ . Then by (16),  $V_L(Z, t) \in B_{\varepsilon_2}$  for all  $t \in [t_d^l, t_d^{l+1})$ .

### V. Case 3

The trajectory of  $V_L$  was in the ball  $B_{\varepsilon_2}$ , and then a switch occurred.

Consider that the trajectory of  $V_L$  was inside the ball  $B_{\varepsilon_2}$  the instant before a switch occurred at time  $t_d^l$ . The Lyapunov function  $V_L$  can only increase so much such that  $V_L(Z(t_d^l), t_d^l) \in B_{\mu^* \varepsilon_2}$  by the definition of  $\mu^*$ , i.e.,  $\frac{W_i(Z(t_d^l), t_d^l)}{W_{i-1}(Z(t_d^l), t_d^l)} \leq \mu^*$ . Using the definition of the dwell-time  $\tau_d^*$ , it can be shown that  $W_i(Z(t_d^l + \tau_d^*), t_d^l + \tau_d^*) \leq \varepsilon_2$ , i.e., the trajectory of  $V_L$  re-enters the ball  $B_{\varepsilon_2}$  before the next switching instance.

Thus, Cases 1–3 together imply that  $\limsup_{t \rightarrow \infty} V_L(Z, t) \leq \mu^* \varepsilon_2$ , where the inequality in (13) guarantees that  $B_{\mu^* \varepsilon_2}$  is contained within the set  $\mathcal{D}$ . Therefore,  $\limsup_{t \rightarrow \infty} \|Z(t)\| \leq \sqrt{\frac{2\mu^* \varepsilon_2}{\min\{\mu^*, 1\}}}$  by the inequalities in (14). Since  $\|x_i - x_L\| \leq \|E\| \leq \|Z\|$  for every  $i \in \mathcal{V}_F$ , we have that  $\limsup_{t \rightarrow \infty} \|x_i(t) - x_L(t)\| \leq \varepsilon \triangleq \mu^* \sqrt{\frac{2}{\psi} \left( \frac{3(\bar{p}^* \bar{N}_d)^2}{k} + 3k (\bar{p}^* \bar{\mathcal{L}}_B (b_{\dot{x}} + \lambda b_x))^2 \right)}$ . An analysis of the closed-loop system shows that the decentralized controller is bounded for all time. ■

*Remark 3:* The expression for the bound of the steady-state convergence error above,  $\varepsilon$ , demonstrates the effect that gain  $k$  has on the convergence error. While the bound on the effects of disturbances from the dynamics can be lowered by increasing the gain  $k$  (similar to many robust control results), the bound on the effect of inaccurate estimates of neighbors' states is exacerbated when increasing the gain  $k$ . This is due to how the difference between the state and the state estimate is effectively multiplied by the gain  $k$  in the control law in (7). Hence, there may be a selection of  $k$  that balances these two effects to minimize the convergence error  $\varepsilon$ , and may be the subject of future research. Furthermore, the expression for the ultimate bound  $\varepsilon$  will increase with greater volatility in the follower agent dynamics or leader trajectory (due to  $\bar{N}_d$ ), inaccuracies between the state and state estimate (due to  $b_x$  and  $b_{\dot{x}}$ ), and topology type (due to  $\bar{p}^*$ ,  $\bar{\mathcal{L}}_B$ , and  $\mu^*$ ). With bounds on the leader trajectory (e.g., planned UAV surveillance area), a bounding expression

for the follower agent dynamics, bounds on state estimate inaccuracies (e.g., anticipated bounds on navigation errors), and knowledge of the topology type, the convergence error bound  $\varepsilon$  may be computed using the bounding techniques described in Section VI. Note that  $\varepsilon$  represents a conservative estimate of the leader-follower state convergence error, where the bound  $\bar{\mathcal{L}}_B$  is especially conservative and may be improved by alternate methods to bound  $\|\mathcal{L}_F(t) + B\|$ . Future efforts may yield an alternative control strategy which can reduce  $\varepsilon$  to be arbitrarily small.

*Remark 4:* The minimum dwell-time used to ensure stability refers to the time that must elapse between any agents' updates. To accomplish this without requiring centralized communication during control implementation, the agents can be pre-programmed with a set of times in which they are allowed to update their consensus weights using a previously computed minimum dwell-time. Section VI addresses how to compute the minimum dwell-time.

Because general nonlinear drift dynamics are considered in Theorem 1, a stabilizing set of initial conditions has to be defined, where the generality of the considered dynamics leads to a stabilizing set of initial conditions and a gain condition that can be difficult to interpret and compute. For clarity in presentation, the following corollary uses a similar proof technique to provide a less conservative result for when globally Lipschitz dynamics (for example, linear dynamics) are considered instead of general nonlinear dynamics. Let  $\Lambda \in \mathbb{R}_{\geq 0}$  be defined as the global Lipschitz constant of  $f_i$  for all  $i \in \mathcal{V}_F$  such that  $\|f_i(y_i) - f_i(y_L)\| \leq \Lambda \|y_i - y_L\|$  for any values of  $y_i, y_L \in \mathbb{R}^m$ , where  $y_i \triangleq [x_i^T \dot{x}_i^T]^T$ ,  $y_L \triangleq [x_L^T \dot{x}_L^T]^T$  such that the two arguments of  $f_i$  are stacked into one argument.

*Corollary 1:* For every follower agent  $i \in \mathcal{V}_F$ , the decentralized controller in (7) using the edge weight update policy in (4) provides uniformly ultimately bounded leader synchronization for a network of agents with globally Lipschitz drift dynamics in the form of (1) with global Lipschitz constant  $\Lambda$ , and neighbor communication and sensing feedback described in Section II-C in the sense that  $\limsup_{t \rightarrow \infty} \|x_i(t) - x_L(t)\| \leq \varepsilon'$  with  $\varepsilon' \triangleq \mu^* \sqrt{\frac{2}{\psi'}} \left( \frac{2\bar{p}^{*2}}{k} \sup_{t \in \mathbb{R}} (\|\dot{x}_L\| + \max_{i \in \mathcal{V}_F} \|f_i(x_L, \dot{x}_L)\|)^2 + 2k (\bar{p}^* \bar{\mathcal{L}}_B (b_{\dot{x}} + \lambda b_x))^2 \right)^{\frac{1}{2}}$  and  $\psi' \triangleq \min \left\{ \lambda - \frac{2}{k} (\bar{p}^* (\Lambda (1 + \lambda) + \lambda^2) + 1)^2, \frac{k}{8} - \bar{p}^* (\Lambda + \lambda) \right\}$ , for any initial conditions of the agents' states, provided that Assumptions 1–4 are satisfied, the dwell-time  $\tau_d$  satisfies  $\tau_d \geq \tau_d^*$ , and the gain  $k$  is selected sufficiently large such that  $k > \max \left\{ \frac{2}{\lambda} (\bar{p}^* (\Lambda (1 + \lambda) + \lambda^2) + 1)^2, 8\bar{p}^* (\Lambda + \lambda) \right\}$ .

*Remark 5:* Similar to the steady-state convergence error bound given in Theorem 1, increasing the gain  $k$  diminishes the bound on the effects of volatility of the follower agents' dynamics and the leader's trajectory; however, the bound on the effect of inaccurate estimates of neighbors' states is exacerbated when increasing the gain  $k$ . While this is only an upper bound on the convergence error, the result suggests that there may be an optimal selection for the gain  $k$ . The discussion in Remark 3 regarding the effects of the leader trajectory, agent dynamics, state estimate inaccuracies, and topology type on the

convergence error  $\varepsilon'$  similarly apply here, where the effects of the agent dynamics on the convergence error are easier to compute due to being globally Lipschitz, i.e., a linear bound can easily be applied. Note that the above conditions are simplified under the assumption of no drift dynamics, i.e.,  $f_i \equiv 0$  for all  $i \in \mathcal{V}_{\mathcal{F}}$ , and thus  $\Lambda = 0$ .

## VI. SATISFACTION OF SUFFICIENT CONDITIONS

In this section, bounds are computed for  $\underline{p}^*$  and  $\bar{p}^*$  so that the size of  $\mathcal{S}$  can be lower-bounded with known information, (13) can be verified, and a value for  $\tau_d$  can be computed which satisfies  $\tau_d \geq \tau_d^*$  (a sufficient condition for convergence in Theorem 1) before the decentralized controller is implemented.

### A. A Lower Bound of $\underline{p}^*$

Using [16, Theorem 3],  $\underline{p}^*$  can be lower-bounded as  $\underline{p}^* \geq \inf_{M \in \mathcal{L}_B} \frac{1}{2\sqrt{\lambda(M^T M)}}$ , where the set  $\mathcal{L}_B$  is defined as the set of all possible values for the matrix  $-\mathcal{L}_{\mathcal{F}} - B$  as  $\mathcal{L}_B \triangleq \{-\mathcal{L}_{\mathcal{F}} - B \mid a_{ij} \in [\underline{a}^*, 1], \sum_{j \in \mathcal{N}_{\mathcal{F}_i}} a_{ij} = 1, \forall (j, i) \in \mathcal{E}_{\mathcal{F}}\}$ . Because  $\sqrt{\lambda(M^T M)} = \|M\| \leq \|M\|_F$  for all  $M \in \mathbb{R}^{\mathcal{F} \times \mathcal{F}}$ , we have that  $\underline{p}^* \geq \inf_{M \in \mathcal{L}_B} \frac{1}{2\|M\|_F} \geq \frac{1}{2\mathcal{L}_B}$ . Thus, a parameter  $\underline{p} \in \mathbb{R}$  can be used to lower bound  $\underline{p}^*$  using known information as  $\underline{p}^* \geq \underline{p} \triangleq \frac{1}{2\sqrt{|\mathcal{E}_{\mathcal{F}}| + \mathcal{F} + \sum_{i \in \mathcal{V}_{\mathcal{F}}} b_i^2}}$ .

### B. An Upper Bound of $\bar{p}^*$

Due to the sensitivity of the CALE (cf. [17, Theorem 8.3.3]), it is difficult to find an analytical upper bound for the norm of the solution of the CALE for an arbitrarily large space of Hurwitz matrices (cf. [18]). An upper bound can easily be computed if the Hurwitz matrix argument is also negative definite (cf. [19]), but the matrix  $-\mathcal{L}_{\mathcal{F}} - B$  may not be negative definite. However, a bound on the perturbation of the solution to the CALE due to a perturbation of the matrix argument can be developed using [17, Theorem 8.3.3] as

$$\frac{\|\Delta \mathcal{P}(M)\|}{\|\mathcal{P}(M) + \Delta \mathcal{P}(M)\|} \leq 2 \|\Delta M\| \|\mathcal{P}(M)\| \quad (19)$$

where  $\Delta \mathcal{P}(M)$  denotes the perturbation of the solution of the CALE for a perturbation of the argument,  $\Delta M$ , such that  $(M + \Delta M)^T (\mathcal{P}(M) + \Delta \mathcal{P}(M)) + (\mathcal{P}(M) + \Delta \mathcal{P}(M))(M + \Delta M) = -I_{\mathcal{F}}$ , where  $M, M + \Delta M$  are Hurwitz matrices. Using (19) and the triangle inequality, a local bound for the perturbation of the solution of the CALE for a given Hurwitz matrix  $M$  can be developed as

$$\|\Delta \mathcal{P}(M)\| \leq \frac{2 \|\Delta M\| \|\mathcal{P}(M)\|^2}{1 - 2 \|\Delta M\| \|\mathcal{P}(M)\|} \quad (20)$$

for all  $\Delta M$  such that  $M + \Delta M$  is Hurwitz and  $\|\Delta M\| < \frac{1}{2\|\mathcal{P}(M)\|}$ . Thus, a natural approach to develop an upper bound for  $\bar{p}^*$  is to iteratively sample in the set  $\mathcal{S}$ , compute an upper bound for the variation of the solution of the CALE in a neighborhood about each sampled point in  $\mathcal{S}$ , continue until the union of the considered neighborhoods covers the space  $\mathcal{S}$ , and use the

---

### Algorithm: 1. Upper bound of $\bar{p}^*$

---

```

v ← 2
p̄ ← max_{M ∈ ℒ_v} 1/(1-φ) ||P(M)||
while min_{M ∈ ℒ_v} φ/(2||P(M)||) < √2 * ((1-a)/(v-1))
  v ← v + 1
  p̄ ← max_{M ∈ ℒ_v} 1/(1-φ) ||P(M)||
end while

```

---

largest upper bound for the solution of the CALE to upper bound  $\bar{p}^*$ . To see that this is possible, consider the following lemma. Let  $\underline{a} \in \mathbb{R}$  be a positive known lower bound of  $\underline{a}^*$ , which can be computed with (2), (4), and  $b_x$  from Assumption 3. Let the set  $\mathcal{L}_B$  be defined as  $\mathcal{L}_B \triangleq \{-\mathcal{L}_{\mathcal{F}} - B \mid a_{ij} \in [\underline{a}, 1] \forall (j, i) \in \mathcal{E}_{\mathcal{F}}\}$ , which is a superset of  $\mathcal{L}_B$  and contains only Hurwitz matrices by Lemma 1. Note that the set  $\mathcal{S}$  is contained within the set  $\{\mathcal{P}(M) \mid M \in \mathcal{L}_B\}$ . Additionally, let the set operator  $\Delta$  be defined as  $\Delta(M) \triangleq \{M + \Delta M \mid (M \in \mathcal{L}_B) \wedge (\Delta M \in \mathbb{R}^{\mathcal{F} \times \mathcal{F}} : \|\Delta M\| \leq \frac{\varphi}{2\|\mathcal{P}(M)\|})\}$ , where  $\varphi \in \mathbb{R}$  satisfies  $0 < \varphi < 1$ .

**Lemma 2:** For any finite selection of matrices  $\{M_1, \dots, M_w\} \in \mathcal{L}_B$ ,  $w \in \mathbb{Z}_{>0}$ , which satisfies  $\bigcup_{n \in \{1, \dots, w\}} \Delta(M_n) \supseteq \mathcal{L}_B$ ,  $\bar{p}^*$  is bounded above by  $\bar{p}^* \leq \max_{n \in \{1, \dots, w\}} \frac{1}{1-\varphi} \|\mathcal{P}(M_n)\|$ .

*Proof:* See the Appendix. ■

Thus, an algorithm to upper bound  $\bar{p}^*$  can be developed which populates the space  $\mathcal{L}_B$  with finitely many  $\{M_1, \dots, M_w\}$  until  $\bigcup_{n \in \{1, \dots, w\}} \Delta(M_n)$  covers  $\mathcal{L}_B$ . The following simple, finite-duration algorithm accomplishes this by creating a uniform mesh of points in (and on the border of) the set  $\mathcal{L}_B$  which is refined until the smallest radius of the closed balls  $\{\Delta(M_1), \dots, \Delta(M_w)\}$  is greater than or equal to the maximum distance between adjacent points in the uniform mesh, thereby covering the set  $\mathcal{L}_B$ . Let the set  $C_v$  be defined as a uniform spacing of  $v \in \mathbb{Z}_{>0}$  ( $v \geq 2$ ) points between  $\underline{a}$  and 1 inclusively such that  $C_v \triangleq \{\alpha_1, \dots, \alpha_v \mid \alpha_i = \underline{a} + \frac{(i-1)(1-\underline{a})}{v-1}\}$ , let  $\mathcal{L}_v$  be defined as the finite set  $\mathcal{L}_v \triangleq \{-\mathcal{L}_{\mathcal{F}} - B \mid a_{ij} \in C_v \forall (j, i) \in \mathcal{E}_{\mathcal{F}}\}$ , and let  $\bar{p} \in \mathbb{R}$  denote an upper bound of  $\bar{p}^*$ .

The while statement condition in Algorithm 1 is developed using an upper bound on the distance (in the sense of the Euclidean norm) between adjacent points in  $\mathcal{L}_v$ . Adjacent points in the set  $\mathcal{L}_v$  differ by a matrix  $\tilde{\mathcal{L}}_v \in \mathbb{R}^{\mathcal{F} \times \mathcal{F}}$  which has  $\pm \frac{1-\underline{a}}{v-1}$  in an off-diagonal entry and  $\pm \frac{1-\underline{a}}{v-1}$  on the diagonal entry of the same row. The distance between adjacent points in  $\mathcal{L}_v$  can then be upper-bounded as  $\|\tilde{\mathcal{L}}_v\| \leq \|\tilde{\mathcal{L}}_v\|_F \leq \sqrt{2 \left(\frac{1-\underline{a}}{v-1}\right)^2}$ . Also, note that a larger selection of the parameter  $\varphi$  can decrease the number of iterations in Algorithm 1, but this may result in a more conservative upper bound for  $\bar{p}^*$ . While this algorithm theoretically terminates in finite operations, it may require too many operations to be feasibly run for a large-sized network. Algorithm 1 is only shown for proof of concept; for actual implementation, a more sophisticated optimization routine may be developed from

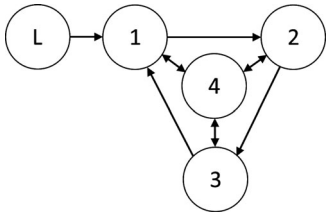


Fig. 1. Network topology.

Algorithm 1, or a more traditional optimization technique can be used to approximate  $\bar{p}^*$  or  $\max \{ \mathcal{P}(M) \mid M \in \mathcal{L}_B \}$ .

### C. Computation of Sufficient Conditions

With the bounding constants  $\underline{p}$  and  $\bar{p}$  that satisfy  $\underline{p} \leq p^*$  and  $\bar{p} \geq \bar{p}^*$ , the size of the set of stabilizing initial conditions  $\mathcal{S}$  can be lower bounded and satisfaction of (13) and  $\tau_d \geq \tau_d^*$  can be guaranteed. Specifically, a conservative estimate  $\underline{\mathcal{S}} \subseteq \mathcal{S}$  can be computed as  $\underline{\mathcal{S}} \triangleq \left\{ Z \in \mathbb{R}^{2\mathcal{F}m} \mid \|Z\| < \frac{\chi}{\mu} \right\}$ , where the constants  $\chi, \mu \in \mathbb{R}$  are defined as  $\chi \triangleq \inf \left( \rho^{-1} \left( \left[ \frac{1}{\bar{p}} \sqrt{\frac{k\psi}{3}}, \infty \right) \right) \right) \in \mathbb{R}$  and  $\mu \triangleq \frac{\max\{\bar{p}, 1\}}{\min\{\underline{p}, 1\}}$ . Additionally, (13) is satisfied if the computable inequality  $\frac{3(\bar{p}\bar{N}_d)^2}{k} + 3k(\bar{p}\bar{\mathcal{L}}_B(b_{\dot{x}} + \lambda b_x))^2 < \frac{\psi\chi}{\mu \max\{\bar{p}, 1\}}$  is satisfied. Finally,  $\tau_d$  can be selected such that  $\tau_d = \frac{\ln(\mu)}{\frac{\psi}{\max\{\bar{p}, 1\}} - \beta}$ , where the tuning parameter  $\beta \in \mathbb{R}$  is selected such that  $0 < \beta < \frac{\psi}{\max\{\bar{p}, 1\}}$ . The inequality  $\tau_d \geq \tau_d^*$  is clearly satisfied if  $\beta^*$  is assigned as  $\beta^* = \beta$ . As with  $\beta^*$ , the selection of  $\beta$  involves a trade-off between convergence rate and the frequency of an agent's edge weight updates.

The estimates  $\underline{p}$  and  $\bar{p}$  may also be used to satisfy the gain condition and approximate the convergence error given in Corollary 1. Note that the methods used to compute the bounds  $\underline{p}$  and  $\bar{p}$  in Sections VI-A and VI-B produce conservative estimates. More sophisticated optimization approaches may yield less conservative bounds and take less computational resources.

## VII. SIMULATION

While the preceding theory guarantees approximate synchronization using the developed reputation-based synchronization method provided that the given sufficient conditions are met, it does not theoretically demonstrate improved convergence time or ultimate synchronization error compared to other methods. A simulation study is performed in this section to compare the performance of the developed reputation-based technique against another reputation-based control technique. The performance of the consensus weight update law given in (2)–(4) with the controller in (7) is demonstrated using the four-agent network depicted in Fig. 1 and the heterogeneous nonlinear dynamics  $\ddot{x}_i = -v_i \|\dot{x}_i\|^2 \begin{bmatrix} \cos(\theta_i) \\ \sin(\theta_i) \end{bmatrix} + u_i$ , which represents a simplified model of a vehicle affected by drag, where the vector  $v = [5.0 \ 5.5 \ 4.5 \ 4.0]^T$  represents the agents' constant drag coefficients, and  $\theta_i$  represents the heading of agent  $i$ , which can be computed using  $\text{atan2}(\dot{x}_{i,2}, \dot{x}_{i,1})$ . The only nonzero

pinning gain is selected as  $b_1 = 3$  and the control gains are selected as  $k = 60$ ,  $\lambda = 20$ . The tuning parameter  $s$  and constant  $\bar{t}$ , used in the trust metric in (2), are selected as  $s = 1$  and  $\bar{t} = 10$  s. The gains used in the reputation algorithm in (3) are selected as  $\eta_{\zeta_i} = 10$ ,  $\eta_{\sigma_i} = 0.1$  for all  $i \in \mathcal{V}_{\mathcal{F}}$ . The simulation is meant to model a real-world scenario in that it is anticipated that the trust values will be lower-bounded as  $\sigma_{ij} \geq 0.2$  for all  $i \in \mathcal{V}_{\mathcal{F}}, j \in \mathcal{N}_{\mathcal{F}i}$ , which, as previously mentioned, implies that  $\zeta_{ij} \geq 0.2$  for all  $i \in \mathcal{V}_{\mathcal{F}}, j \in \mathcal{N}_{\mathcal{F}i}$ . The MATLAB optimization routine `fmincon` is executed to obtain estimates of  $\underline{p}^*$  and  $\bar{p}^*$  using the gains  $k$  and  $\lambda$ , the network topology depicted in Fig. 1, the pinning gain  $b_1$ , and the bounds  $0.2 \leq \zeta_{ij} \leq 1$ , resulting in the estimates  $\underline{p} = 0.119$  and  $\bar{p} = 8.28$ . The dwell-time for the consensus weight updates is then computed as  $\tau_d = 2.4$  s using the assignment  $\beta = 0.001 \frac{2\psi}{\max\{\bar{p}, 1\}}$ . The agents' onboard sensor equipment is modeled to have a frequency of 20 Hz, where at each sensor measurement an agent has a 50% chance of sensing a neighbor. Only one neighbor can be observed in a single sensor measurement, and the neighbor seen is a random selection, where each neighbor is equally likely to be seen. The onboard position estimates are modeled to be affected by an offset such that  $\hat{x}_i = x_i + \Delta x_i$ , where  $\Delta x_1 = [1 \ 1]^T$ ,  $\Delta x_2 = [-1 \ -1]^T$ ,  $\Delta x_3 = [0.5 \ \sin(t)]^T$ , and  $\Delta x_4 = \begin{cases} [-0.5 \ -0.5]^T & \text{if } t < 60 \\ (90 + 30 \sin(7t)) [1 \ 1]^T & \text{if } t \geq 60 \end{cases}$ . Thus, agents 1-4 have very accurate (but not perfect) estimates of their position from 0-60 s. After 60 s, the position estimate maintained by agent 4 becomes very inaccurate, which may be due to onboard localization sensor failure, for example. The onboard velocity estimates are similarly affected as  $\hat{\dot{x}}_i = \dot{x}_i + \frac{d}{dt}(\Delta x_i)$ . The network-wide objective is to track the leader state trajectory, which evolves as  $x_L = [\sin(t) \ 0.5 \cos(t)]^T$ .

To demonstrate the benefit of updating the consensus weights based on reputation, consensus weights are updated after the closed-loop system has come to steady-state. The first update occurs at 120 s and the agents' updates are staggered in time in intervals of  $\tau_d$ . The benefit of the consensus weight updates is shown in the plot of the leader-tracking error in Fig. 2, where the leader-tracking error of agent 4 is high due to its very inaccurate state estimate, and is therefore omitted. The tracking error of agent 1 is less affected by the inaccurate position and velocity estimates of agent 4 since agent 1 is directly connected to the leader; however, the effects of agent 4 percolate through the network and severely worsen the tracking performance of agents 2 and 3, as shown in Fig. 2. The deleterious effects of agent 4 are mitigated by the trust measurements, neighbor reputations, and consensus weight updates, shown in Figs. 3–5. Upon achieving steady-state using consensus weight updates, the leader-tracking errors return to values similar to those obtained when agent 4 had very accurate position estimates.

Note that the trust values went below the anticipated lower bound of 0.2, where the lower bound 0.2 was used to compute the update dwell-time. However, the closed-loop system is still stable, which emphasizes the fact that the given conditions are only sufficient, and lower dwell-times than  $\tau_d$  may also provide stability.

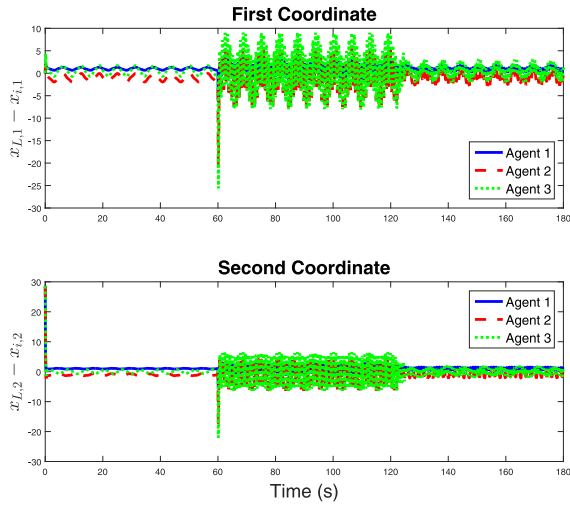


Fig. 2. Leader-tracking error.

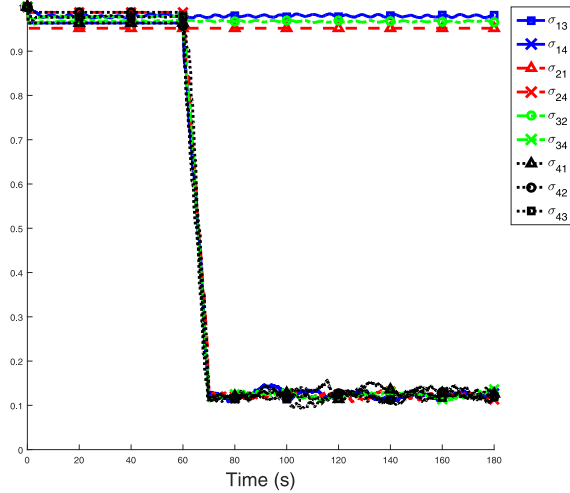


Fig. 3. Trust measurements.

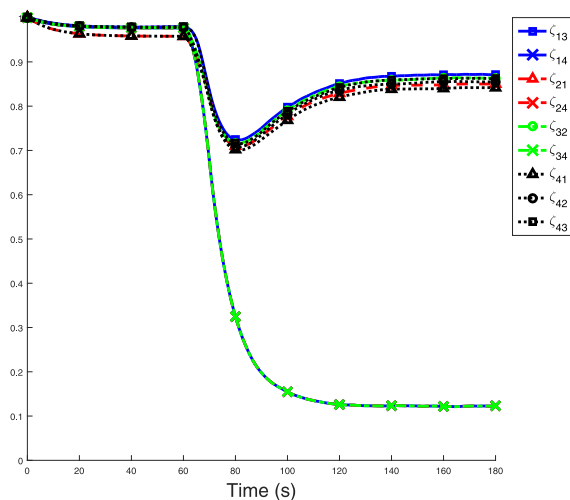


Fig. 4. Neighbor reputations.

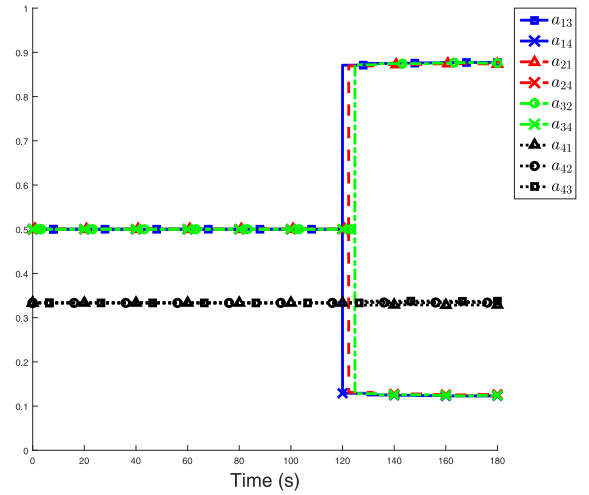


Fig. 5. Dynamically updated consensus (adjacency) weights.

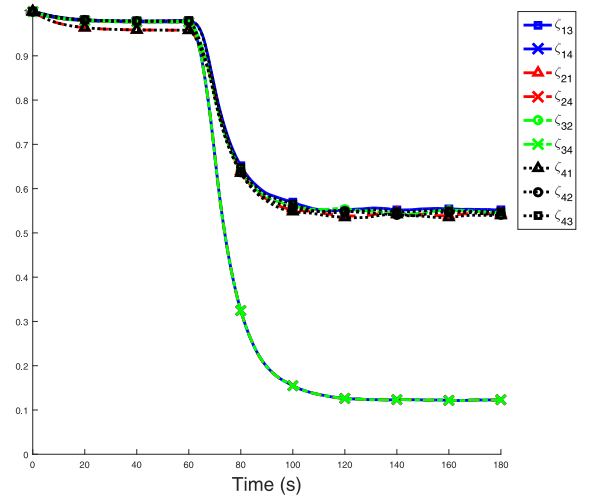


Fig. 6. Neighbor reputations produced by the alternative reputation algorithm in (21).

The benefit of weighting the contributions of neighbor recommendations based on their reputations, seen by the multiplication by  $\zeta_{in}$  in (3), is demonstrated by performing the simulation again without the multiplicative term  $\zeta_{in}$  in (3). The resulting reputation algorithm that omits  $\zeta_{in}$ , shown in (21), resembles the reputation algorithm given in [10], where  $\zeta'_{ij}$  denotes the alternative reputation measure obtained with the algorithm in (21).

$$\zeta'_{ij} = \sum_{n \in \mathcal{N}_{\mathcal{F}_i} \cap \mathcal{N}_{\mathcal{F}_j}} \eta_{\zeta i} (\zeta'_{nj} - \zeta'_{ij}) + \eta_{\sigma i} (\sigma_{ij} - \zeta'_{ij}) \quad (21)$$

The simulation results show that, compared to the results obtained using the reputation algorithm in (3), the reputation algorithm in (21) produces 19.7% worse leader-tracking performance in terms of the RMS leader tracking error magnitudes summed across each agent (i.e.,  $\sum_{i \in \{1,2,3\}} \text{rms} \|x_L - x_i\|$ ) from 160 to 180 seconds (i.e., steady state, after updates to the consensus weights began). The neighbor reputations for this second simulation are shown in Fig. 6, where the

reputations of well-localized agents,  $\zeta_{21}, \zeta_{32}, \zeta_{13}$ , are lower compared to the results produced by the reputation algorithm in (3). The reputations are diminished because the recommendation by agent 4 is not weighted by the reputation of agent 4, unlike in the algorithm in (3).

### VIII. CONCLUSION

A decentralized controller and reputation algorithm which updates consensus weights were developed for approximate synchronization to the leader agent's state, where the reputation algorithm uses the discrepancy between unreliable communicated information and intermittent neighbor sensing data of a neighbor agent in collaboration with mutual neighbors. The leader-follower network topology is modeled as strongly-connected and static, but the updates of consensus weights produce a switched system. Approximate synchronization is ensured through a Lyapunov-based stability analysis and techniques from switching control theory, which help develop a dwell-time for the follower agents' consensus weight updates. Whereas most switched control approaches develop a dwell-time based on a finite number of possible structures for the closed-loop dynamics, the dwell-time discussed in this work is based on bounds of the minimum and maximum eigenvalues of the solution to the CALE over a space of Hurwitz matrices due to the infinite number of possible combinations of the network consensus weights; to the authors' knowledge, this technique is novel.

Some exciting results may be extended from this research. In particular, these developments can be extended to devise more sophisticated context-dependent reputation algorithms, an augmentation to the decentralized controller which decides when to sever neighbor connections, and an observer which determines a more accurate estimate of neighbors' states given unreliable communication and accurate intermittent neighbor sensing. Additionally, while communication of inaccurate position information could be considered as malicious instead of unintentional in the framework considered in this paper, the convergence analysis assumes that each agent follows the prescribed decentralized control law, which keeps the agents from being considered completely malicious. Similar to [9], future research may address consideration of fully malicious agents in the design of a reputation algorithm.

### APPENDIX

*Proof of Lemma 1:* By Assumption 1 and [20, Lemma 4.6], the left eigenvector  $p = [p_1, \dots, p_{\mathcal{F}}]^T \in \mathbb{R}^{\mathcal{F}}$  of  $\mathcal{L}_{\mathcal{F}}$  associated with the (simple) zero eigenvalue has all positive entries. Let  $\xi = [\xi_1, \dots, \xi_{\mathcal{F}}]^T \in \mathbb{R}^{\mathcal{F}} \setminus \{\mathbf{0}\}$ , where  $\mathbf{0}$  denotes the origin of the appropriate dimension. Because  $p^T \mathcal{L}_{\mathcal{F}} = \mathbf{0}$ , we have that  $p_i d_i = \sum_{j=1}^{\mathcal{F}} p_j a_{ji}$ , and hence  $\sum_{j=1}^{\mathcal{F}} p_i a_{ij} = \sum_{j=1}^{\mathcal{F}} p_j a_{ji}$  for all  $i \in \mathcal{V}_{\mathcal{F}}$ , which gives the relation

$$\begin{aligned} & \sum_{i=1}^{\mathcal{F}} \sum_{j=1}^{\mathcal{F}} p_i a_{ij} \xi_i (\xi_i - \xi_j) \\ &= \sum_{i=1}^{\mathcal{F}} \sum_{j=1}^{\mathcal{F}} p_i a_{ij} \xi_i^2 - \sum_{i=1}^{\mathcal{F}} \sum_{j=1}^{\mathcal{F}} p_i a_{ij} \xi_i \xi_j \end{aligned}$$

$$\begin{aligned} &= \sum_{i=1}^{\mathcal{F}} \sum_{j=1}^{\mathcal{F}} p_j a_{ji} \xi_i^2 - \sum_{i=1}^{\mathcal{F}} \sum_{j=1}^{\mathcal{F}} p_i a_{ij} \xi_i \xi_j \\ &= \sum_{i=1}^{\mathcal{F}} \sum_{j=1}^{\mathcal{F}} p_i a_{ij} \xi_j^2 - \sum_{i=1}^{\mathcal{F}} \sum_{j=1}^{\mathcal{F}} p_i a_{ij} \xi_i \xi_j \\ &= \sum_{i=1}^{\mathcal{F}} \sum_{j=1}^{\mathcal{F}} p_i a_{ij} \xi_j (\xi_j - \xi_i). \end{aligned} \quad (22)$$

Let  $Q \in \mathbb{R}^{\mathcal{F} \times \mathcal{F}}$  be defined as  $Q \triangleq P(\mathcal{L}_{\mathcal{F}} + B) + (\mathcal{L}_{\mathcal{F}} + B)^T P$ , where  $P \triangleq \text{diag}\{p_1, \dots, p_{\mathcal{F}}\} \in \mathbb{R}^{\mathcal{F} \times \mathcal{F}}$ . The relation in (22) facilitates the expression of the product  $\xi^T Q \xi$  as

$$\begin{aligned} \xi^T Q \xi &= \xi^T P \mathcal{L}_{\mathcal{F}} \xi + \xi^T \mathcal{L}_{\mathcal{F}}^T P \xi + \xi^T P B \xi + \xi^T B P \xi \\ &= 2 \xi^T P \mathcal{L}_{\mathcal{F}} \xi + 2 \xi^T P B \xi \\ &= 2 \sum_{i=1}^{\mathcal{F}} \sum_{j=1}^{\mathcal{F}} p_i \xi_i a_{ij} (\xi_i - \xi_j) + 2 \sum_{i=1}^{\mathcal{F}} p_i b_i \xi_i^2 \\ &= \sum_{i=1}^{\mathcal{F}} \sum_{j=1}^{\mathcal{F}} p_i a_{ij} \xi_i (\xi_i - \xi_j) + \sum_{i=1}^{\mathcal{F}} \sum_{j=1}^{\mathcal{F}} p_i a_{ij} \xi_j (\xi_j - \xi_i) \\ &\quad + 2 \sum_{i=1}^{\mathcal{F}} p_i b_i \xi_i^2 \\ &= \sum_{i=1}^{\mathcal{F}} \sum_{j=1}^{\mathcal{F}} p_i a_{ij} (\xi_j - \xi_i)^2 + 2 \sum_{i=1}^{\mathcal{F}} p_i b_i \xi_i^2. \end{aligned}$$

Clearly,  $\xi^T Q \xi \geq 0$ . Suppose that  $\xi^T Q \xi = 0$  for some  $\xi \in \mathbb{R}^{\mathcal{F}} \setminus \{\mathbf{0}\}$ , which requires that  $\sum_{i=1}^{\mathcal{F}} \sum_{j=1}^{\mathcal{F}} p_i a_{ij} (\xi_j - \xi_i)^2 = 0$  and  $\sum_{i=1}^{\mathcal{F}} p_i b_i \xi_i^2 = 0$ . Because  $\mathcal{G}_{\mathcal{F}}$  is strongly connected and  $\xi \in \mathbb{R}^{\mathcal{F}} \setminus \{\mathbf{0}\}$ ,  $\sum_{i=1}^{\mathcal{F}} \sum_{j=1}^{\mathcal{F}} p_i a_{ij} (\xi_j - \xi_i)^2 = 0$  if and only if  $\xi = \alpha \mathbf{1}_{\mathcal{F}}$ , where  $\alpha \in \mathbb{R} \setminus \{0\}$  and  $\mathbf{1}_{\mathcal{F}} \in \mathbb{R}^{\mathcal{F}}$  denotes a vector of ones. However, if at least one follower agent is connected to the leader, then  $\sum_{i=1}^{\mathcal{F}} p_i b_i \xi_i^2 > 0$  for all  $\xi \in \text{span}\{\mathbf{1}_{\mathcal{F}}\} \setminus \{\mathbf{0}\}$ , which results in a contradiction. Hence,  $\xi^T Q \xi > 0$  for all  $\xi \in \mathbb{R}^{\mathcal{F}} \setminus \{\mathbf{0}\}$ , i.e.,  $Q$  is positive definite. Therefore, because  $P$  is positive definite and symmetric and the matrix  $P(-\mathcal{L}_{\mathcal{F}} - B) + (-\mathcal{L}_{\mathcal{F}} - B)^T P$  is negative definite by the definition of  $Q$ , we have by [21, Theorem 8.2] that  $-\mathcal{L}_{\mathcal{F}} - B$  is Hurwitz.

*Proof of Lemma 2:* Because  $\sup\{\|\mathcal{P}(M)\| \mid M \in \bar{\mathcal{L}}_B\}$  is bounded, the ball  $\Delta(M)$  is non-vanishing for any  $M \in \bar{\mathcal{L}}_B$ . Additionally, because  $\sup\{\|\mathcal{P}(M)\| \mid M \in \bar{\mathcal{L}}_B\}$  is bounded,  $\mathcal{P}$  is continuous in the non-vanishing neighborhood  $\Delta(M) \cap \bar{\mathcal{L}}_B$  for every  $M \in \bar{\mathcal{L}}_B$  by (20), which implies that  $\mathcal{P}$  is continuous over  $\bar{\mathcal{L}}_B$ . Hence, because  $\mathcal{P}$  is continuous over  $\bar{\mathcal{L}}_B$  and  $\bar{\mathcal{L}}_B$  is compact, the set  $\{\mathcal{P}(M) \mid M \in \bar{\mathcal{L}}_B\}$  is compact, and therefore there exists a matrix  $M_0 \in \bar{\mathcal{L}}_B$  such that  $\|\mathcal{P}(M)\| \leq \|\mathcal{P}(M_0)\|$  for every  $M \in \bar{\mathcal{L}}_B$ . Thus, for any finite selection of matrices  $\{M_1, \dots, M_w\} \in \bar{\mathcal{L}}_B$  which satisfy

$\cup_{n \in \{1, \dots, w\}} \Delta(M_n) \supseteq \bar{\mathcal{L}}_B$ , we have that

$$\begin{aligned} \bar{p}^* &\leq \|\mathcal{P}(M_0)\| \\ &\leq \max_{n \in \{1, \dots, w\}} \max_{\Delta M \in \Delta(M_n)} (\|\mathcal{P}(M_n + \Delta M)\|) \\ &= \max_{n \in \{1, \dots, w\}} \max_{\Delta M \in \Delta(M_n)} (\|\mathcal{P}(M_n) + \Delta \mathcal{P}(M_n)\|) \\ &\leq \max_{n \in \{1, \dots, w\}} \frac{1}{1 - \varphi} \|\mathcal{P}(M_n)\| \end{aligned}$$

by the fact that  $\mathcal{P} \subset \{\mathcal{P}(M) \mid M \in \bar{\mathcal{L}}_B\}$ , the definition of  $\Delta(\cdot)$ , the upper bound in (20), and the triangle inequality. Note that  $\|\Delta \mathcal{P}(M_n)\|$  is kept bounded by introducing  $\varphi$  in the definition of  $\Delta$  to keep the denominator in (20) from being arbitrarily close to zero.

## REFERENCES

- [1] A. Rodriguez-Angeles and H. Nijmeijer, "Mutual synchronization of robots via estimated state feedback: A cooperative approach," *IEEE Trans. Control Syst. Technol.*, vol. 12, no. 4, pp. 542–554, 2004.
- [2] W. Ren, "Multi-vehicle consensus with a time-varying reference state," *Syst. Control Lett.*, vol. 56, pp. 474–483, 2007.
- [3] E. Nuño, R. Ortega, L. Basañez, and D. Hill, "Synchronization of networks of nonidentical Euler-Lagrange systems with uncertain parameters and communication delays," *IEEE Trans. Autom. Control*, vol. 56, no. 4, pp. 935–941, 2011.
- [4] J. R. Klotz, Z. Kan, J. M. Shea, E. L. Pasilio, and W. E. Dixon, "Asymptotic synchronization of a leader-follower network of uncertain Euler-Lagrange systems," *IEEE Trans. Control Netw. Syst.*, vol. 2, no. 2, pp. 174–182, 2014.
- [5] J. Klotz, R. Kamalapurkar, and W. E. Dixon, "Concurrent learning-based network synchronization," in *Proc. Amer. Control Conf.*, 2014, pp. 796–801.
- [6] X. Liu and J. S. Baras, "Using trust in distributed consensus with adversaries in sensor and other networks," in *Proc. IEEE 17th Int. Conf. Inf. Fusion*, Jul. 2014, pp. 1–7.
- [7] D. G. Mikulski, F. L. Lewis, E. Y. Gu, and G. R. Hudas, "Trust method for multi-agent consensus," in *Proc. SPIE*, vol. 8387, May 2012.
- [8] P. Ballal, F. L. Lewis, and G. R. Hudas, *Recent Advances in Nonlinear Dynamics and Synchronization*. New York: Springer, 2009, ch. Trust-based collaborative control for teams in communication networks, pp. 347–363.
- [9] H. LeBlanc, H. Zhang, S. Sundaram, and X. Koutsoukos, "Consensus of multi-agent networks in the presence of adversaries using only local information," in *Proc. 1st Int. Conf. High Confid. Netw. Syst.*, New York, 2012, pp. 1–10.
- [10] T. Haus, I. Palunko, D. Tolić, S. Bogdan, and F. L. Lewis, "Decentralized trust-based self-organizing cooperative control," in *Proc. IEEE Eur. Control Conf.*, Strasbourg, France, 2014, pp. 1205–1210.
- [11] B. Khosravifar, M. Gomrokchi, and J. Bentahar, "Maintenance-based trust for multi-agent systems," in *Proc. 8th Int. Joint Conf. Auton. Agents Multiagent Syst.*, vol. 2, Budapest, Hungary, 2009, pp. 1017–1024.
- [12] K. Govindan and P. Mohapatra, "Trust computations and trust dynamics in mobile adhoc networks: A survey," *IEEE Commun. Surv. Tutor.*, vol. 14, no. 2, pp. 279–298, 2012.
- [13] D. Liberzon, *Switching in Systems and Control*. Basel, Switzerland: Birkhauser, 2003.
- [14] R. Kamalapurkar, J. A. Rosenfeld, J. Klotz, R. J. Downey, and W. E. Dixon, "Supporting lemmas for RISE-based control methods," *arXiv:1306.3432v3*, 2014.
- [15] H. K. Khalil, *Nonlinear Systems*, 3rd ed. Upper Saddle River, NJ: Prentice Hall, 2002.
- [16] J. J. Montemayor and B. F. Womack, "Comments on "on the Lyapunov matrix equation"," *IEEE Trans. Autom. Control*, vol. AC-20, no. 6, pp. 814–815, 1975.
- [17] B. N. Datta, *Numerical Methods for Linear Control Systems: Design and Analysis*. London, U.K.: Elsevier Academic Press, 2004.
- [18] M. Konstantinov, D.-W. Gu, V. Mehrmann, and P. Petkov, *Perturbation Theory for Matrix Equations*, ser. Studies in Computational Mathematics, C. K. Chui, P. Mond, and L. Wuytack, Eds. Elsevier, 2003, vol. 9.
- [19] S.-D. Wang, T.-S. Kuo, and C.-F. Hsu, "Trace bounds on the solution of the algebraic matrix Riccati and Lyapunov equation," *IEEE Trans. Autom. Control*, vol. AC-31, no. 7, pp. 654–656, 1986.
- [20] E. Semsar-Kazerooni and K. Khorasani, *Team Cooperation in a Network of Multi-Vehicle Unmanned Systems: Synthesis of Consensus Algorithms*. New York: Springer, 2013.
- [21] J. P. Hespanha, *Linear Systems Theory*. Princeton, NJ: Princeton University Press, 2009.



**Justin R. Klotz** received the Ph.D. degree in mechanical engineering from the University of Florida, Gainesville, in 2015, where he was awarded the Science, Mathematics and Research for Transformation (SMART) Scholarship, sponsored by the Department of Defense.

His research interests include the development of Lyapunov-based techniques for reinforcement learning-based control, switching control methods, delay-affected control, and trust-based cooperative control.



**Anup Parikh** received the B.S. degree in mechanical and aerospace engineering, the M.S. degree in mechanical engineering, and the Ph.D. in aerospace engineering from the University of Florida, Gainesville.

Currently, he is a Postdoctoral Researcher at Sandia National Laboratories, Albuquerque, NM. His primary research interests include Lyapunov-based control and estimation theory and application in autonomous systems.



**Teng-Hu Cheng** received the Ph.D. degree from the Department of Mechanical Engineering, University of Florida, in 2015, under the supervision of Dr. Dixon.

In 2016, he joined National Chiao Tung University in the Department of Mechanical Engineering. His research interests include networked system control, switched control, event-driven control, and nonlinear control.



**Warren E. Dixon** (F'16) received the Ph.D. degree from Clemson University, Clemson, South Carolina, in 2000.

He is a Newton C. Ebaugh Professor of Mechanical and Aerospace Engineering at the University of Florida, Gainesville. His main research interest has been the development and application of Lyapunov-based control techniques for uncertain nonlinear systems. His work has resulted in various early career and best paper awards.

Dr. Dixon is also a Fellow of ASME.